IOSR Journal of Mechanical and Civil Engineering (IOSR-JMCE)
e-ISSN: 2278-1684, p-ISSN: 2320-334X, Volume 22, Issue 4 Ser. 1 (Jul. – Aug. 2025), PP 47-55
www.iosrjournals.org

TOPSIS-Based Suitability Ranking of Aluminosilicate Precursors for Geopolymer Applications from Oxide Composition Analysis

[1*]Ohwerhi, Kelly Erhiferhi, [1]Aghaebene, Isah Nwabenu, [1]Nwaobakata, Chukwuemeka
[1] Department of Civil Engineering, University of Port Harcourt, Port Harcourt, Nigeria
** Corresponding Author; Ohwerhi Kelly Erhiferhi (kellyohwerhi@gmail.com)*

Abstract
Reducing carbon emissions from Portland cement production has accelerated interest in geopolymer technology as a sustainable binder alternative. This study evaluates and ranks three aluminosilicate precursors, metakaolin (MK), rice husk ash (RHA), and periwinkle shell ash (PSA), based on their oxide compositions critical to geopolymerization: silica (SiO_2), alumina (Al_2O_3), calcium oxide (CaO), and iron oxide (Fe_2O_3). X-ray fluorescence (XRF) analysis quantified these oxides, and the Technique for Order of Preference by Similarity to Ideal Solution (TOPSIS) was applied for systematic ranking, with oxide weights set as SiO_2 (40%), Al_2O_3 (30%), CaO (20%), and Fe_2O_3 (10%). MK demonstrated the most balanced composition, 60.24% SiO_2, 23.54% Al_2O_3, low CaO (4.67%) and Fe_2O_3 (1.56%), favoring strong sodium aluminosilicate hydrate (N-A-S-H) gel formation. RHA had high silica content (83.39%) but low alumina (2.13%), limiting its standalone geopolymer potential. PSA's high calcium (38.85%) suggests formation of calcium-aluminosilicate hydrate (C-A-S-H) phases, less ideal for pure geopolymer gels. TOPSIS ranking identified MK as the most suitable precursor (Ci = 0.7851), followed by RHA (0.5442) and PSA (0.3021). This oxide-based, multi-criteria evaluation framework provides a replicable protocol for selecting geopolymer precursors, enabling sustainable mix design and promoting broader adoption of low-carbon construction materials.*

Keywords; TOPSIS, Precursors, Aluminosilicates, Geopolymer, Oxide Composition

Date of Submission: 07-07-2025 Date of Acceptance: 17-07-2025

I. Introduction

The urgent need to reduce the carbon emissions associated with Portland cement production has spurred the exploration of geopolymer technology as a sustainable alternative. Globally, the cement industry is responsible for approximately 7–8% of anthropogenic CO_2 emissions, primarily due to calcination of limestone and energy-intensive clinker production (Scrivener et al., 2018). In contrast, geopolymer binders are synthesized by activating aluminosilicate-rich precursors, such as metakaolin, fly ash, or agricultural waste ashes, with alkaline solutions, resulting in materials that exhibit excellent chemical resistance, high thermal stability, and significantly reduced carbon footprints (Lahoti et al., 2017; Provis & Bernal, 2014). The precursor material critically influences the overall reactivity, microstructural development, and mechanical performance of the geopolymer matrix. For instance, metakaolin is noted for its high purity and reactivity, leading to dense and durable geopolymer structures (Adesanya & Ohenoja, 2021), while rice husk ash and periwinkle shell ash, as agro-industrial by-products, offer sustainability advantages and a viable source of reactive silica and alumina (Rovnaník et al., 2021; Olutoge et al., 2020). Therefore, precursor selection remains a fundamental aspect of geopolymer mix design, especially when balancing environmental, mechanical, and economic performance criteria.

Among various aluminosilicate sources, metakaolin is widely regarded as a benchmark precursor due to its high purity and reactivity, which results from the thermal activation of kaolinite clay at temperatures typically between 650°C and 800°C (Lahoti et al., 2017; Palomo et al., 2014). The oxide composition of metakaolin is typically dominated by silica (SiO_2) and alumina (Al_2O_3), accounting for more than 90% of its mass, which are critical components for the formation of the geopolymer gel network that imparts mechanical strength and durability (Davidovits, 2015; Bernal et al., 2012). Despite these favorable properties, the high energy consumption associated with the calcination process, alongside the relatively limited natural deposits of kaolinite in some geographic regions, presents challenges to its large-scale, sustainable application (De Silva et al., 2017; Liew et al., 2017). Consequently, there is growing interest in exploring alternative aluminosilicate precursors such as fly ash, rice husk ash, volcanic ash, and shell-derived ashes that are more regionally abundant,

DOI: 10.9790/1684-2204014755

cost-effective, and environmentally friendly (Shah et al., 2020; Rovnaník et al., 2021). These alternatives, however, often require additional processing or blending to achieve comparable reactivity and performance to metakaolin-based geopolymers (Adesanya & Ohenoja, 2021).

Rice husk ash (RHA) has emerged as a promising agro-waste-derived precursor for geopolymer synthesis due to its high silica content and amorphous structure. When rice husks are combusted under controlled conditions—typically between 500°C and 700°C—the resulting ash contains more than 80% amorphous silica, which exhibits excellent reactivity in alkaline environments necessary for geopolymerization (Muhammad et al., 2021; Singh et al., 2019). This high silica content facilitates the dissolution and polymerization processes that form the aluminosilicate gel network, resulting in geopolymer matrices with satisfactory mechanical properties such as compressive strength and durability (Olutoge & Adesina, 2019; Anwar et al., 2020). Moreover, using RHA as a precursor aligns with circular economy principles by valorizing agricultural waste, reducing landfill disposal, and lowering the environmental footprint of construction materials (Kumar et al., 2020; Muhammad et al., 2021). The utilization of RHA thus not only enhances sustainability but also provides a cost-effective alternative to conventional geopolymer precursors like metakaolin and fly ash.

Another emerging precursor is periwinkle shell ash (PSA), derived from calcined marine shell waste, which is gaining attention due to its unique chemical composition and sustainability potential. Although less extensively studied than metakaolin and rice husk ash, PSA contains significant amounts of silica (SiO_2), alumina (Al_2O_3), and calcium oxide (CaO), which are key oxides contributing to the formation of both sodium aluminosilicate hydrate (N-A-S-H) geopolymer gels and calcium aluminosilicate hydrate (C-A-S-H) hybrid gels (Aboshio et al., 2018; Olutoge et al., 2020). The coexistence of these phases can enhance the mechanical strength and durability of the resulting binder, providing a potential advantage over pure N-A-S-H geopolymers. Research incorporating PSA in cementitious and geopolymer matrices has demonstrated improvements in compressive strength, resistance to chemical attack, and reduced environmental impact through valorization of marine biomass waste (Aboshio et al., 2018; Ogedengbe et al., 2021). Thus, PSA represents a promising sustainable alternative that can contribute to circular economy principles while diversifying the pool of geopolymer precursors.

The primary oxides of interest in geopolymer precursor evaluation are silica (SiO_2), alumina (Al_2O_3), calcium oxide (CaO), and iron oxide (Fe_2O_3), as these largely govern the formation, structure, and stability of the geopolymeric aluminosilicate networks. Silica and alumina serve as the essential building blocks for the formation of the three-dimensional geopolymer gel, typically sodium aluminosilicate hydrate (N-A-S-H), which imparts mechanical strength and chemical durability (Provis & Bernal, 2014; Davidovits, 2015). The presence of calcium oxide contributes to the development of calcium aluminosilicate hydrate (C-A-S-H) gel phases, which are known to enhance early-age strength and densify the microstructure (Gao et al., 2020; Puertas et al., 2014). However, while moderate CaO content can be beneficial, excessive calcium levels may lead to rapid precipitation of C-A-S-H gels that interfere with the formation of the amorphous geopolymer network, potentially causing reduced workability and long-term durability issues (Muhammad et al., 2021; Kong & Sanjayan, 2010). Similarly, iron oxide (Fe_2O_3) can influence the geopolymerization process, where low to moderate levels may contribute to structural stability, but higher contents might disrupt gel homogeneity or color, and affect mechanical performance negatively (Duxson et al., 2007; Muhammad et al., 2021). Therefore, a balanced oxide composition in precursor materials is critical to optimizing geopolymer performance.

Although numerous studies have extensively evaluated the mechanical performance of geopolymer binders synthesized from a variety of aluminosilicate precursors, there remains a relative paucity of research that focuses specifically on oxide composition as a fundamental metric for precursor suitability. Most existing studies emphasize performance outcomes such as compressive strength, durability, or workability under varied curing conditions, activator types, and mix proportions (Lahoti et al., 2017; Adesanya & Ohenoja, 2021). However, a chemically focused approach centered on the quantification and balance of primary oxides, such as SiO_2, Al_2O_3, CaO, and Fe_2O_3, offers a more intrinsic and transferable basis for evaluating and comparing precursor materials across different processing conditions (Provis & Bernal, 2014; Rovnaník et al., 2021). This fundamental perspective facilitates precursor ranking and mix design optimization independent of external variables like curing regime, activator concentration, or specimen geometry, thus enabling more consistent and predictive geopolymer formulation strategies (Davidovits, 2015; Muhammad et al., 2021). Such an approach supports the development of standardized criteria for precursor evaluation, accelerating the adoption of sustainable materials in construction.

Therefore, this study aims to evaluate and rank the suitability of three aluminosilicate precursors, metakaolin, rice husk ash, and periwinkle shell ash, for geopolymer applications based exclusively on their oxide composition. The investigation emphasizes the relative proportions of key oxides, silica (SiO_2), alumina (Al_2O_3), calcium oxide (CaO), and iron oxide (Fe_2O_3), as these fundamentally govern the geopolymerization process, gel formation, and resulting material properties. To achieve a systematic and objective ranking, the Technique for Order of Preference by Similarity to Ideal Solution (TOPSIS) is employed as a multi-criteria decision-making tool, incorporating oxide content weights based on their functional importance. By integrating TOPSIS into the evaluation framework, this research provides a replicable and chemically grounded protocol for precursor selection, facilitating sustainable geopolymer mix design and broader adoption of low-carbon construction materials.

II. Materials and Methods

2.1 Materials

Kaolin, commonly referred to as white clay, was sourced from a natural deposit located in Agbaghara Nsu, within the Ehime Mbano Local Government Area of Imo State, Nigeria, at coordinates 5.6649° N, 7.3030° E. A visual representation of the collected kaolin sample is provided in Figure 1. To produce metakaolin for use as a geopolymer precursor in this study, the raw kaolin underwent a series of processing steps.

First, the kaolin was oven-dried for approximately 48 hours to eliminate residual moisture and ensure a dry, workable material. The dried clay was then subjected to thermal activation by calcining it at a temperature of 700 °C for 120 minutes in a locally fabricated muffle furnace, capable of reaching up to 1400 °C. This calcination process transformed the kaolin into metakaolin, a highly reactive, amorphous aluminosilicate.

Subsequently, the calcined metakaolin was ground into fine powder and passed through a No. 200 sieve (75 µm). Only the fraction that passed through the sieve was used in the experimental procedures, ensuring particle size uniformity and optimal reactivity in the geopolymer matrix.

The resulting metakaolin exhibited a specific gravity of 2.52, reflecting its relatively dense composition. Its density also suggests a substantial contribution to the compactness and mechanical strength of resulting geopolymer binder, as supported by the findings of Mehta and Siddique (2017).

Figure 1. Sourced Kaolin Sample

Waste periwinkle shells were locally sourced from an assemblage of discarded shells in Aluu, Port Harcourt, Nigeria. To obtain periwinkle shell ash (PSA) suitable for use as a geopolymer precursor, the collected shells underwent a systematic processing sequence.

Initially, the periwinkle shells were thoroughly washed to remove dirt and impurities, then sun-dried for 48 hours to eliminate residual moisture. Following this, the dried shells were calcined at approximately 800 °C in a muffle furnace until they turned whitish and brittle, an indication of successful thermal transformation.

The calcined shells were then pulverized using a grinding machine to produce a fine powder. This powder was subjected to sieve analysis, and only the fraction passing through a No. 200 sieve (75 µm) was retained for experimental use, ensuring a consistent and reactive particle size distribution.

The resulting periwinkle shell ash exhibited a specific gravity of 2.46, which is slightly lower than that of metakaolin. Despite this, the relatively high density of PSA indicates its potential to contribute to the compactness and mechanical strength of geopolymer binders.

Powdered rice husk ash (RHA), derived from waste rice husk calcined at 450 °C, was procured from a reliable supplier based in Benue State, Nigeria. The RHA was delivered in 25 kg rice bags and, upon receipt, was subjected to sieve analysis to ensure particle size uniformity. Only the fraction passing through a No. 200 sieve (75 μm) was utilized for the experimental program, as finer particles are more reactive and contribute more effectively to geopolymer formation.

The RHA recorded the lowest specific gravity among the aluminosilicate precursors used in this study, with a value of 2.07. This relatively low specific gravity is indicative of its porous structure and lower particle density, characteristics typical of ash-based materials. The lower density of RHA suggests a beneficial influence on the workability of geopolymer mixtures, potentially improving flowability while also reducing the overall mass of the hardened product.

Such properties are particularly advantageous in the production of lightweight geopolymers, where a balance between reduced weight and adequate mechanical performance is essential. As noted by Kumar and Kumar (2011), the use of porous, low-density materials like RHA can enhance the versatility and sustainability of geopolymer applications in structural and non-structural contexts.

2.2 Methods

2.2.1 Oxide Composition Analysis

The oxide compositions of metakaolin (MK), periwinkle shell ash (PSA), and rice husk ash (RHA) were determined using the X-ray fluorescence (XRF) method, following the procedures outlined in ASTM D8064-16 (2016). This analysis was carried out at the AUSTINO Laboratory located in Alakahia, Rivers State. In the course of this study, attention was focused on four primary oxides: silica (SiO_2), alumina (Al_2O_3), calcium oxide (CaO), and iron oxide (Fe_2O_3). These oxides were selected deliberately due to their central role in geopolymer chemistry, their dominant presence in common aluminosilicate sources, and their well-established influence on the performance characteristics of geopolymer binders.

Silica and alumina are the two principal components responsible for the geopolymerization process. The interaction between silicate and aluminate species under alkaline conditions forms the basis of the geopolymer matrix, primarily consisting of sodium aluminosilicate hydrate (N-A-S-H) or, in calcium-rich systems, calcium-aluminosilicate hydrate (C-A-S-H). The Si/Al molar ratio significantly affects the gel structure, mechanical strength, and durability of the resulting geopolymer. Therefore, assessing the concentrations of SiO_2 and Al_2O_3 in the precursor materials is critical for determining their suitability for geopolymer applications.

Calcium oxide (CaO), although not traditionally associated with pure geopolymers, plays a significant role when present in moderate quantities. It contributes to the formation of C-A-S-H gel, which can coexist with N-A-S-H phases, thereby enhancing early strength development and improving the material's resistance to moisture and chemical degradation. This makes CaO particularly important when evaluating precursors such as PSA, which may naturally contain higher levels of calcium due to their biological origin.

Iron oxide (Fe_2O_3) is another relevant component, often present in varying quantities in aluminosilicate materials. While its role is less direct than that of silica or alumina, Fe_2O_3 can partially substitute for Al_2O_3 in the geopolymeric framework, particularly under low-silica conditions. Its presence influences both the microstructural development and the long-term stability of the geopolymer binder. In addition, iron oxide can affect the color and chemical durability of the material, especially when used in aggressive environments.

The decision to limit the analysis to these four oxides was also informed by practical considerations. These oxides are routinely reported in the literature as key indicators of geopolymer precursor quality. Focusing on them simplifies the screening process and allows for direct comparison with previously published data. Other oxides, such as magnesium oxide (MgO), sodium oxide (Na_2O), and potassium oxide (K_2O), though present in trace amounts, typically have minimal influence unless found in substantial proportions. Their exclusion helps streamline the analysis without compromising its relevance or accuracy.

2.2.2 Technique for Order of Preference by Similarity to Ideal Solution (TOPSIS) for Precursor Suitability Ranking

The TOPSIS method is based on the concept that the most suitable alternative is the one closest to the ideal solution and farthest from the negative ideal solution, measured using Euclidean distance. In this study, the alternatives refer to the three aluminosilicate precursors, which are evaluated and ranked according to their oxide compositions. The assessment is guided by four key performance indicators, SiO_2, Al_2O_3, CaO, and Fe_2O_3. These criteria form the basis for comparing the alternatives. As outlined by Yoon and Hwang (1995), the procedure involves the following steps:

1. **Decision Matrix;** The decision matrix is formulated as presented by Equation (1). Each row represents a precursor, and each column represents an oxide (e.g., SiO_2, Al_2O_3, CaO, Fe_2O_3).

$$D = \begin{bmatrix} d_{11} & d_{12} & d_{13} & d_{14} \\ d_{21} & d_{22} & d_{23} & d_{24} \\ d_{31} & d_{32} & d_{33} & d_{34} \end{bmatrix} \qquad (1)$$

Where; D = Decision matrix

d_{ij} = denotes the performance value of precursor d_i under criterion c_j.

2. **Normalized Decision Matrix**; Normalized decision matrix is presented by Equation (2), where, normalization ensures that all values in the transformed matrix fall within the range [0, 1], while preserving the relative magnitude of the original data.

$$R = \begin{bmatrix} r_{11} & r_{12} & r_{13} & r_{14} \\ r_{21} & r_{22} & r_{23} & r_{24} \\ r_{31} & r_{32} & r_{33} & r_{34} \end{bmatrix} \qquad (2)$$

Where: r_{ij} is the normalized value of d_{ij}, which was obtained on application of Equation (3).

$$r_{ij} = \frac{d_{ij}}{\sqrt{\sum_{i=1}^{m} d_{ij}^2}} \qquad (3)$$

Where: r_{ij} is the normalized value of d_{ij}; d_{ij} is the original value in the decision matrix, m is the number of alternatives, and $\sum_{i=1}^{m} d_{ij}^2$ is the sum of the squared values for criterion Cj

3. **Weighted- Normalized Decision Matrix;** In this study, the relative importance assigned to each oxide was as follows: 40% for SiO_2, 30% for Al_2O_3, 20% for CaO, and 10% for Fe_2O_3. Consequently, the weight vector is defined as W = [0.4, 0.3, 0.2, 0.1], which is then applied to transform the normalized decision matrix (D) into the weighted normalized matrix (V), as described in Equation (4).

$$V = \begin{bmatrix} v_{11} = r_{11} * 0.4 & v_{12} = r_{12} * 0.3 & v_{13} = r_{13} * 0.2 & v_{14} = r_{14} * 0.1 \\ v_{21} = r_{21} * 0.4 & v_{22} = r_{22} * 0.3 & v_{23} = r_{23} * 0.2 & v_{24} = r_{24} * 0.1 \\ v_{31} = r_{31} * 0.4 & v_{32} = r_{32} * 0.3 & v_{33} = r_{33} * 0.2 & v_{34} = r_{34} * 0.1 \end{bmatrix} \quad (4)$$

Where: v_{ij} is the weighted value for precursor, f_i under criterion cj, r_{ij} is the normalized value from the previous step, ensuring that $\sum_{j=1}^{n} w_j = 1$.

4. **Ideal and Negative Ideal Solutions**: In TOPSIS, decision-makers identify an ideal solution (best-case scenario) and a negative ideal solution (worst-case scenario). These solutions serve as benchmarks against each alternative is evaluated. The formulas for determining these solutions depend on the type of criterion:

$$V^+ = \{\max v_{ij} \,|j \in B, \min v_{ij}|\, j \in C\} \qquad (5)$$

$$V^- = \{\min v_{ij} \,|j \in B, \max v_{ij}|\, j \in C\} \qquad (6)$$

Where: B represents benefit criteria such as SiO_2 and Al_2O_3 (higher values are preferred), C represents cost criteria such as CaO and Fe_2O_3 (lower values are preferred). Thus, for each criterion, if it is a benefit criterion (B), the ideal solution takes the maximum value, and the negative ideal solution takes the minimum value. If it is a cost criterion (C), the ideal solution takes the minimum value, and the negative ideal solution takes the maximum value.

5. **Separation Measures**; After determining the ideal solution (V^+) and the negative ideal solution (V^-), separation measures were determined using Equation (7).

$$S_i^+ = \sqrt{\sum_{j=1}^{n} \left(v_{ij} - v_j^+\right)^2} \qquad (7a)$$

$$S_i^- = \sqrt{\sum_{j=1}^{n} \left(v_{ij} - v_j^-\right)^2} \qquad (7b)$$

Where: Si^+ is the distance of factor fi from the ideal solution, Si^- is the distance of factor fi from the negative ideal solution, v_{ij} is the weighted value of factor fi under criterion Cj, vj^+ and vj^- are the ideal and negative ideal values for criterion Cj, respectively.

6. **Relative Closeness and Ranking Alternatives**; next, is to compute the relative closeness coefficient (Ci^*). This coefficient quantifies how close each factor is to the ideal solution relative to the negative ideal solution. The relative closeness coefficient (Ci^*) was computed using Equation (8).

$$C_i^* = \frac{S_i^-}{S_i^+ + S_i^-} \qquad (8)$$

Where: Si^+ is the distance from the ideal solution (lower is better), Si^- is the distance from the negative ideal solution (higher is better), Ci^* ranges between 0 and 1, where a higher value indicates a better alternative. After computing Ci^* for each alternative, the alternatives are ranked in descending order based on their closeness coefficient.

III.Results and Discussion

3.1 Oxide Composition of Precursors

Figure 1 illustrates the oxide composition profiles of the three geopolymer precursors under investigation: metakaolin (MK), periwinkle shell ash (PSA), and rice husk ash (RHA). The results reveal that MK possesses a high proportion of silica and alumina, comprising approximately 60.24% SiO_2 and 23.54% Al_2O_3, along with 4.67% CaO and 1.56% Fe_2O_3. This chemical profile classifies MK as a highly reactive aluminosilicate, making it well-suited for geopolymer synthesis. The relatively balanced content of silica and alumina enhances the development of a strong aluminosilicate network, which is essential for geopolymer gel formation (Duxson et al., 2007; Rashad, 2013). The low levels of calcium and iron further support MK's classification as a low-calcium geopolymer precursor, conducive to forming sodium aluminosilicate hydrate (N-A-S-H) gels rather than calcium-dominant hydrates.

In contrast, PSA demonstrated a markedly different oxide distribution, with 34.55% SiO_2, 11.04% Al_2O_3, a significantly elevated 38.85% CaO, and 5.3% Fe_2O_3. The high calcium content suggests that PSA behaves more like a cementitious or hybrid material than a classic geopolymer precursor. Such calcium-rich materials tend to promote the formation of calcium-silicate-hydrate (C-S-H) rather than the N-A-S-H gel networks typically associated with alkali-activated aluminosilicates (Provis & Bernal, 2014; Abubakar et al., 2021). While PSA may exhibit partial pozzolanic behavior, its high CaO concentration can interfere with the polymerization of silica and alumina species, thereby limiting its effectiveness as a stand-alone geopolymer precursor.

RHA, on the other hand, exhibited an exceptionally high silica content (83.39% SiO_2), with very low levels of Al_2O_3 (2.13%), CaO (1.07%), and Fe_2O_3 (1.32%). This composition characterizes RHA as a siliceous pozzolan. Its high amorphous silica content enables strong reactivity with alkaline activators; however, the low alumina content poses a limitation for geopolymer synthesis, as a sufficient quantity of Al_2O_3 is necessary to form the three-dimensional aluminosilicate structure (Chindaprasirt et al., 2007; Mehta et al., 2022). Therefore, although RHA can serve as a potent silica source, it typically requires blending with an alumina-rich material like MK to achieve an optimal Si/Al ratio for effective geopolymer gel development.

Overall, these findings highlight the chemical diversity among the precursors and underscore the need for compositional balance, particularly in terms of SiO_2 and Al_2O_3, when designing geopolymer systems. The oxide-based analysis serves as a practical screening tool for selecting suitable materials for sustainable geopolymer binder production.

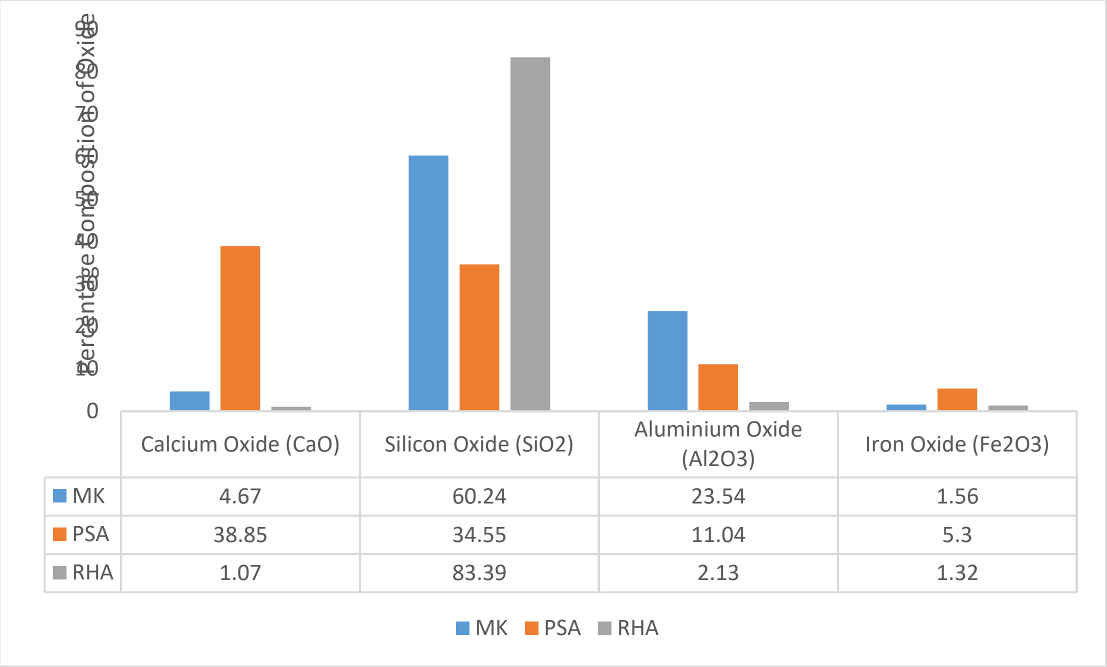

	Calcium Oxide (CaO)	Silicon Oxide (SiO2)	Aluminium Oxide (Al2O3)	Iron Oxide (Fe2O3)
■ MK	4.67	60.24	23.54	1.56
■ PSA	38.85	34.55	11.04	5.3
■ RHA	1.07	83.39	2.13	1.32

Figure 1. Oxide Composition Results of Precursors

3.2 TOPSIS Analysis for Proper Ranking of Precursors

3.2.1 Formulation of Decision Matrix

The decision matrix is formulated as presented by Equation (9). The decision matrix for oxide composition analysis of the precursors is a 3 X 4 matrix, where, 3 represents the number of precursors, and 4 represents the performance parameters.

$$D = \begin{bmatrix} MK_{Sio2} = 60.24 & MK_{Al2O3} = 23.54 & MK_{CaO} = 4.67 & MK_{Fe2O3} = 1.56 \\ PSA_{Sio2} = 34.55 & PSA_{Al2O3} = 11.04 & PSA_{CaO} = 38.85 & PSA_{Fe2O3} = 5.30 \\ RHA_{Sio2} = 83.39 & RHA_{Al2O3} = 2.13 & RHA_{CaO} = 1.07 & RHA_{Fe2O3} = 1.32 \end{bmatrix} \quad (9)$$

3.2.2 Formulation of Normalized Decision Matrix

With the aid of Equations (2) and (3), the normalized decision matrix is obtained as presented by Equation (10). Normalization ensures that all values in the transformed matrix fall within the range [0, 1], while preserving the relative magnitude of the original data

$$R = \begin{bmatrix} 0.5553 & 0.9025 & 0.1193 & 0.2748 \\ 0.3184 & 0.4233 & 0.9926 & 0.9331 \\ 0.7686 & 0.0816 & 0.0273 & 0.2325 \end{bmatrix} \qquad (10)$$

3.2.3 Formulation of Weighted-Normalized Matrix

For this study, SiO_2 was given a weight of 0.4 (40%), 30% for Al_2O_3, 20% for CaO, and 10% for Fe_2O_3. Thus, the weight vector becomes, W = [0.4, 0.3, 0.2, 0.1], modifying the normalized decision matrix R to the weighted-normalized matrix, V (Equation 11). Equation (11), therefore represents the weighted-normalized decision matrix.

$$V = \begin{bmatrix} 0.2221 & 0.2708 & 0.0239 & 0.0275 \\ 0.1274 & 0.1270 & 0.1985 & 0.0933 \\ 0.3075 & 0.0245 & 0.0055 & 0.0233 \end{bmatrix} \qquad (11)$$

3.2.4 Determination of Ideal and Negative Ideal Solutions

Because both SiO_2 and Al_2O_3 are benefit-related criteria and CaO and Fe2O3 are cost-related criteris, Equations (5) and (6) were applied to determine the ideal and negative ideal solutions. Equation (12), thus represents the ideal and negative ideal solutions.

Ideal solution; $V^+ = [0.3075; 0.2708;\ 0.0055;\ 0.0233]$ (12a)

Negative ideal solution; $V^- = [0.1274; 0.0245;\ 0.1985;\ 0.0933]$ (12b)

3.2.5 Determination of Separation Measures

Separation measures, S_i^+ and S_i^- were determined with the aid of using Equation (7) together with Equations (12) and (11). This results to the final separation measures as presented in Equation (13).

$$S^* = \begin{bmatrix} Precursor & S^+ & S^- \\ MK & 0.0886 & 0.3233 \\ PSA & 0.3088 & 0.1025 \\ RHA & 0.2463 & 0.2733 \end{bmatrix} \qquad (13)$$

3.2.6 Determination of Relative Closeness for Ranking of Precursors

Using Equations (8) and (13), the relative closeness coefficient (Ci∗) for each precursor is determined, as expressed in Equation (14). Based on the rankings in Equation (14), MK with a relative closeness of 0.7851 ranks highest, making it the most suitable for geopolymer applications. This is followed by RHA with a relative closeness of 0.5253 and lastly PSA with a relative closeness of 0.2496.

$$C^* = \begin{bmatrix} Precursor & C & Rank \\ MK & 0.7851 & 1st \\ PSA & 0.2496 & 3rd \\ RHA & 0.5253 & 2nd \end{bmatrix} \qquad (14)$$

According to the results, metakaolin (MK) achieved the highest relative closeness value of 0.7851, positioning it as the most suitable candidate for geopolymer applications. This high score reflects MK's well-balanced chemical composition, especially its high content of reactive silica and alumina, which are critical for effective geopolymerization. Prior studies have affirmed the superior performance of MK-based geopolymers, citing their enhanced mechanical strength, durability, and thermal resistance (Duxson et al., 2007; Rashad, 2013).

Rice husk ash (RHA) ranked second with a closeness coefficient of 0.5253. Although RHA is exceptionally rich in amorphous silica, essential for geopolymer gel formation, its relatively low alumina content limits its standalone applicability in geopolymer synthesis. To overcome this limitation, RHA is often blended with alumina-rich materials like MK to optimize the Si/Al ratio and enhance the reactivity of the system (Mehta et al., 2022; Chindaprasirt et al., 2007).

In contrast, periwinkle shell ash (PSA) recorded the lowest relative closeness value of 0.2496, indicating its limited suitability as a geopolymer precursor. This is attributed primarily to its high calcium oxide (CaO) content, which tends to favor the formation of calcium-silicate-hydrate (C-S-H) phases rather than the aluminosilicate network characteristic of geopolymers (Provis & Bernal, 2014; Abubakar et al., 2021). While PSA may contribute pozzolanic reactivity in blended systems, its dominance of CaO undermines its effectiveness in alkali-activated binder systems where N-A-S-H gels are preferred.

The computed Ci* values therefore provide a rational and replicable basis for ranking precursor materials based on their oxide compositions, offering practical insights for material selection in sustainable geopolymer production.

IV.Conclusions

In the search for sustainable alternatives to conventional cementitious binders, geopolymer technology has emerged as a promising solution. The performance of geopolymer systems is strongly influenced by the chemical composition of the precursor materials, particularly the contents of silicon dioxide (SiO_2), aluminum oxide (Al_2O_3), calcium oxide (CaO), and iron oxide (Fe_2O_3). This study comparatively evaluates the oxide compositions of three potential precursors, Metakaolin (MK), Periwinkle Shell Ash (PSA), and Rice Husk Ash (RHA) using TOPSIS, a multi-criteria decision-making method. The goal is to establish a robust, replicable ranking of precursor suitability for geopolymer synthesis based on quantitative oxide data;

i. Metakaolin (MK) exhibits the most favorable oxide composition with high SiO_2 (60.24%) and Al_2O_3 (23.54%), making it ideal for N-A-S-H gel formation in geopolymer synthesis. Rice Husk Ash (RHA) is rich in SiO_2 (83.39%) but lacks sufficient Al_2O_3 (2.13%), limiting its standalone geopolymer potential. Periwinkle Shell Ash (PSA) has high CaO (38.85%) and moderate SiO_2 and Al_2O_3, classifying it as more suitable for C-S-H gel formation than for true geopolymerization. Overall, MK is best suited for geopolymer use, while RHA and PSA may serve as supplementary materials.

ii. The TOPSIS analysis, based on weighted oxide parameters, ranked metakaolin (MK) highest with a relative closeness coefficient of 0.7851 due to its balanced and geopolymer-friendly oxide composition. Rice husk ash (RHA) followed with a score of 0.5253, benefiting from its high silica content but limited by low alumina. Periwinkle shell ash (PSA) ranked lowest at 0.2496, primarily because its high calcium content favors C-S-H formation over geopolymerization. These rankings confirm MK as the most suitable precursor, while RHA and PSA may serve as supplementary or blended materials.

iii. The oxide-based screening provides a practical and replicable method for selecting suitable precursors in geopolymer design. By quantifying and ranking precursor suitability, the study offers valuable guidance for optimizing mix designs based on chemical composition. The successful application of the TOPSIS method highlights its effectiveness in multi-criteria decision-making for sustainable material selection. This approach supports more informed and strategic choices in geopolymer research and eco-friendly construction practices.

REFERENCES

[1]. Aboshio, M. A., Olutoge, F. A., & Oke, A. O. (2018). Effects of periwinkle shell ash as partial replacement of cement on the strength and durability of concrete. Case Studies in Construction Materials, 8, 127–134. https://doi.org/10.1016/j.cscm.2017.12.001

[2]. Abubakar, M., Lawal, A. I., & Farouk, A. (2021). Chemical and microstructural evaluation of periwinkle shell ash blended cement. Case Studies in Construction Materials, 15, e00640. https://doi.org/10.1016/j.cscm.2021.e00640

[3]. Adesanya, E., & Ohenoja, K. (2021). Reactivity and performance of metakaolin-based geopolymers: Effects of synthesis parameters and precursor characteristics. Construction and Building Materials, 283, 122748. https://doi.org/10.1016/j.conbuildmat.2021.122748

[4]. Anwar, M. P., Kumar, R., & Singh, B. (2020). Rice husk ash based geopolymer concrete: A review on synthesis, properties, and potential applications. Construction and Building Materials, 243, 118200. https://doi.org/10.1016/j.conbuildmat.2020.118200

[5]. ASTM International. (2016). ASTM D8064-16: *Standard test method for elemental analysis of soil and solid waste by monochromatic energy dispersive X-ray fluorescence spectrometry using multiple monochromatic excitation beams*. ASTM International. https://doi.org/10.1520/D8064-16

[6]. Bernal, S. A., Provis, J. L., Walkley, B., San Nicolas, R., Gehman, J. D., Brice, D. G., Kilcullen, A. R., Duxson, P., & Van Deventer, J. S. J. (2012). Gel nanostructure in alkali-activated materials. Applied Clay Science, 88–89, 209–218. https://doi.org/10.1016/j.clay.2013.01.005

[7]. Chindaprasirt, P., Jaturapitakkul, C., & Sinsiri, T. (2007). Use of rice husk ash to improve the mechanical properties and sulfate resistance of cement mortars. Construction and Building Materials, 21(7), 1709–1714. https://doi.org/10.1016/j.conbuildmat.2006.05.005

[8]. Davidovits, J. (2015). Geopolymer chemistry and applications (4th ed.). Institut Géopolymère.

[9]. De Silva, P., Sagoe-Crentsil, K., & Sirivivatnanon, V. (2017). Kinetics of geopolymerization: Role of Al_2O_3 and SiO_2. Cement and Concrete Research, 37(4), 512–518. https://doi.org/10.1016/j.cemconres.2006.01.004

[10]. Duxson, P., Fernández-Jiménez, A., Provis, J. L., Lukey, G. C., Palomo, A., & van Deventer, J. S. J. (2007). Geopolymer technology: The current state of the art. Journal of Materials Science, 42, 2917–2933. https://doi.org/10.1007/s10853-006-0637-z

[11]. Duxson, P., Provis, J. L., Lukey, G. C., & Van Deventer, J. S. J. (2007). The role of inorganic polymer technology in the development of 'green concrete'. Cement and Concrete Research, 37(12), 1590–1597. https://doi.org/10.1016/j.cemconres.2007.07.018

[12]. Gao, X., Zhang, X., & Zhu, Z. (2020). Effects of CaO on the mechanical and microstructural properties of metakaolin-based geopolymers. Construction and Building Materials, 262, 120602. https://doi.org/10.1016/j.conbuildmat.2020.120602

[13]. Kong, D., & Sanjayan, J. G. (2010). Damage behavior of geopolymer composites exposed to elevated temperature. Cement and Concrete Composites, 32(4), 269–274. https://doi.org/10.1016/j.cemconcomp.2010.01.005

[14]. Kumar, S., Ali, A., Ahmad, F., & Rashid, M. (2020). Utilization of agricultural wastes for sustainable geopolymer production: A review. Journal of Cleaner Production, 267, 122034. https://doi.org/10.1016/j.jclepro.2020.122034

[15]. Lahoti, M., Wong, L. S., & Yang, E. H. (2017). Geopolymer cement concretes: A review of recent developments. Construction and Building Materials, 154, 926–944. https://doi.org/10.1016/j.conbuildmat.2017.08.038

[16]. Liew, K. M., Zhang, L., Mo, K. H., & Yan, C. (2017). Sustainable geopolymer composites for construction applications. Materials, 10(8), 960. https://doi.org/10.3390/ma10080960

[17]. Mehta, A., & Siddique, R. (2017). An overview of geopolymers derived from industrial by-products. *Construction and Building Materials*, 127, 183-198. https://doi.org/10.1016/j.conbuildmat.2016.09.136

[18]. Mehta, A., Siddique, R., & Jamshed, M. A. (2022). Utilization of rice husk ash in geopolymer binders and concretes: A comprehensive review. Construction and Building Materials, 343, 128090. https://doi.org/10.1016/j.conbuildmat.2022.128090

[19]. Muhammad, S., Bakhsh, K., & Khan, K. (2021). Influence of combustion temperature on the properties of rice husk ash for geopolymer applications. Journal of Environmental Chemical Engineering, 9(1), 104606. https://doi.org/10.1016/j.jece.2020.104606

[20]. Ogedengbe, O. T., Olutoge, F. A., & Akinmade, E. A. (2021). Sustainable utilization of periwinkle shell ash in cementitious composites: Microstructure and mechanical performance evaluation. Journal of Cleaner Production, 291, 125924. https://doi.org/10.1016/j.jclepro.2020.125924

[21]. Olutoge, F. A., & Adesina, A. A. (2019). Experimental study on the influence of rice husk ash and other pozzolanic materials on the properties of geopolymer concrete. Materials Today: Proceedings, 16, 2350–2355. https://doi.org/10.1016/j.matpr.2019.06.073

[22]. Olutoge, F. A., Adesanya, E., & Amusan, T. V. (2020). Performance evaluation of periwinkle shell ash blended with rice husk ash as a sustainable cementitious material in concrete. Case Studies in Construction Materials, 13, e00434. https://doi.org/10.1016/j.cscm.2020.e00434

[23]. Olutoge, F. A., Adewale, A. A., & Adenuga, A. H. (2020). Mechanical properties and durability performance of periwinkle shell ash blended cement concrete. Construction and Building Materials, 230, 117017. https://doi.org/10.1016/j.conbuildmat.2019.117017

[24]. Palomo, A., Grutzeck, M. W., & Blanco, M. T. (2014). Alkali-activated fly ashes: A cement for the future. Cement and Concrete Research, 29(8), 1323–1329. https://doi.org/10.1016/S0008-8846(99)00114-6

[25]. Provis, J. L., & Bernal, S. A. (2014). Geopolymers and related alkali-activated materials. Annual Review of Materials Research, 44, 299–327. https://doi.org/10.1146/annurev-matsci-070813-113515

[26]. Puertas, F., Fernández-Jiménez, A., & Blanco-Varela, M. T. (2014). Cement and concrete research: Alkali-activated cementitious materials: Past, present and future. Cement and Concrete Research, 55, 211–222. https://doi.org/10.1016/j.cemconres.2013.10.001

[27]. Rashad, A. M. (2013). Metakaolin as cementitious material: History, scours, production and composition – A comprehensive overview. Construction and Building Materials, 41, 303–318. https://doi.org/10.1016/j.conbuildmat.2012.12.001

[28]. Rovnaník, P., Šafránková, K., & Bayer, P. (2021). Characterization of rice husk ash and its application in alkali-activated binders. Materials, 14(10), 2503. https://doi.org/10.3390/ma14102503

[29]. Scrivener, K. L., John, V. M., & Gartner, E. M. (2018). Eco-efficient cements: Potential economically viable solutions for a low-CO_2 cement-based materials industry. Cement and Concrete Research, 114, 2–26. https://doi.org/10.1016/j.cemconres.2018.03.015

[30]. Shah, S. F. A., Ali, T., Alam, F., Abbas, S., Nawaz, W., & Nazari, A. (2020). Fly ash-based geopolymer concrete: A review of recent advancements and sustainable construction. Construction and Building Materials, 260, 119844. https://doi.org/10.1016/j.conbuildmat.2020.119844

[31]. Singh, B., Ishwarya, G., Gupta, M., & Bhattacharyya, S. K. (2019). Influence of synthesis parameters on microstructure and mechanical properties of rice husk ash based geopolymer concrete. Construction and Building Materials, 202, 295–307. https://doi.org/10.1016/j.conbuildmat.2019.01.064